SEDIMENTOLOGY the journal of the International Association of Sedimentologists

Sedimentology (2016) doi: 10.1111/sed.12289

Sedimentary characteristics of palaeolake deposits along the Indus River valley, Ladakh, Trans-Himalaya: Implications for the depositional environment

DEBARATI NAG*, BINITA PHARTIYAL* and DHRUV SEN SINGH†
*Birbal Sahni Institute of Palaeosciences, 53 University Road, Lucknow, UP 226007, India (E-mail: binitaphartiyal@gmail.com)
†Department of Geology, Lucknow University, Lucknow, UP 226007, India

Associate Editor – Daniel Ariztegui

ABSTRACT

This study is an attempt to contribute to the data set of granulometric studies of sediments by measuring the sedimentary structure and texture, along with statistical parameters, of cold and arid lake systems. The palaeolake sequence along the River Indus on the western fringe of the Tibetan Plateau in Ladakh sector was selected in order to shed light on depositional environmental changes within the lake from post-last glacial maximum to 5 ka. The River Indus was blocked by Lamayuru dam burst during the deglaciation, after the Last Glacial Maximum (LGM) and the subsequent increase in water level led to the formation of the Saspol–Khalsi palaeolake. This lake was *ca* 55 km in length, extending from Nimo to Khalsi, had a surface area of 370 km^2 and was in existence until 5 ka. Two sections (Saspol and Khalsi) separated by an aerial distance of 35 km show a similar trend in sediment character due to their deposition in the same lake system. Grain-size studies show a polymodal nature of sediments for both of the sections. However, sediments of the lower/downstream section (Khalsi) show a poorer degree of sorting, and coarser grain size and high energy depositional condition as compared with the sediments of Saspol section (positioned upstream) due to the location of the sections within the lake system. It was noted that, in high-altitude arid regions, the sedimentological characteristics of large-sized valley lakes may vary greatly, horizontally as well as vertically, owing to local stream input, inflow intensity from the catchment, outflow velocity of water channels, lithology and valley widths at the different sites.

Keywords Cold deserts, granulometry, Ladakh, palaeolakes, Trans-Himalaya.

INTRODUCTION

Lakes are dynamic systems that integrate environmental, climatic and tectonic forcing into continuous high resolution archives of local and regional scale (Gierlowski-Kordesch & Kelts, 2000). There are more than 300 lakes having a surface area greater than 10 km^2 on the Tibetan Plateau, and the total lake surface area exceeds 40 000 km^2 at present (Wang & Dou, 1998). Several lakes in this cold high-altitude desert are dry (palaeo) and several others are showing signs of low water levels, while some are dry completely. Lake expansion and/or shrinkage in this region result from changing precipitation and evaporation controlled by the strength of Asian monsoons and the Westerlies (Bookhagen *et al.*, 2005; Chen *et al.*, 2008; Long *et al.*, 2012). Tibetan lakes have experienced significant changes in water level since the LGM (Gasse *et al.*, 1991), inferred mainly from lacustrine sediment records (Gasse *et al.*, 1991, 1996; van Campo & Gasse,

1993; Gu *et al.*, 1993; Wei & Gasse, 1999; Wu *et al.*, 2006; Mügler *et al.*, 2010) and the chronostratigraphy of lake terraces (Long *et al.*, 2010). This suggestion is supported by field surveys which show that many Tibetan lakes are surrounded by multiple palaeo-shorelines (Zhao *et al.*, 2003; Zheng *et al.*, 2006; Lee *et al.*, 2009; Kong *et al.*, 2011) and stacks of lacustrine deposits along the river valleys (Sangode *et al.*, 2011, 2013; Phartiyal *et al.*, 2013, 2015; Blöthe *et al.*, 2014; Nag & Phartiyal, 2015). These shorelines and the palaeo-lacustrine deposits provide information on the timing and volume of former high lake levels, as well as the ancient/past lake extent and environment. Thus, the spatial and temporal changes of these lakes can be studied (Lee *et al.*, 2009) and linked to climate history. Based on the elevation of the highest shoreline, it was proposed that an extensive ancient lake system existed in central Tibet (Lehmkuhl & Haselein, 2000). If the high lake level of major lakes occurred at the same time, the total lake area could have been as large as 150 000 km^2, and this assumption has led to the pan-lake hypothesis (Zheng *et al.*, 2006).

Lakes in the Ladakh region are of two types; closed basins and open basins. Most of the palaeo-lakes reported so far from the vicinity of the Indus Suture Zone (ISZ) and Karakorum Fault (KF; Phartiyal *et al.*, 2005, 2013, 2015; Sangode *et al.*, 2011; Sant *et al.*, 2011; Nag & Phartiyal, 2015) are valley lakes, formed by the blockage of the river drainage due to tectonic or climatic effects or a combination of both. Several lakes of the region are well-studied: Lamayuru lake (Fort *et al.*, 1989; Sangode & Bagati, 1995; Bagati *et al.*, 1996; Kotlia *et al.*, 1997a,b, 1998; Shukla *et al.*, 2002) and Tsokar lake for lake morphology, sedimentation and palaeoclimate (Demske *et al.*, 2009; Wünnemann *et al.*, 2010); Tso Morairi for endogenic carbonates as a climate-proxy (Mishra *et al.*, 2015); and Pangong Tso for fluctuating lake levels and climate (Fontes *et al.*, 1996; Gasse *et al.*, 1996; Hui *et al.*, 1996; Phartiyal *et al.*, 2015). Being a cold desert, much of the sediment debris lies loose on the high angled slopes and is likely to block the river at its narrow stretch even with a slight climatic or tectonic perturbation, thereby forming a hydrographically closed basin with an inlet and outlet of the main drainage. It has long been observed that sediments generated by similar kinds of geological and environmental conditions should have similar grain-size distribution properties (Udden, 1914; Inman & Chamberlain, 1955; Mason & Folk, 1958; Spencer, 1963; Sahu, 1964; Folk, 1966; Visher, 1969; Reineck & Singh, 1973; Glaister & Nelson, 1974; Bagnold & Barndorff-Nielsen, 1980; Håkanson & Jansson, 1983; Boggs, 1995; Reading & Levell, 1996). Therefore, analysis of lake sediments can reflect an overall hydrodynamic condition at the site of deposition.

The present study deals with the sediment characterization of a palaeolake that existed along the Indus River valley, formed as a consequence of impoundment. This Trans-Himalayan region of Ladakh comprises numerous glacial (Pulu and Tsoltak) and saline lakes (Tsokar and Pangong Tso) stretching from a few square metres to hundreds of square kilometres in area and also as palaeolake deposits well-preserved along the present day river channels. The Saspol–Khalsi palaeolake, which dates to 14·6 to 5·0 ka (Nag & Phartiyal, 2015), is evidence of a valley lake caused by impoundment along the River Indus by climatic and tectonic disturbances which was later drained out due to the same activities. In this study, the grain-size distribution of this palaeolake sediment is used as a proxy to interpret the hydrological conditions associated with climatic changes that existed at that time. The sedimentary texture and structure along with statistical parameters of every litho-unit of the two sections (separated by a distance of *ca* 35 km) have been worked out to obtain an idea of the macro and micro-depositional environment from this high altitude cold arid region of the world. About one-third of the land surface of the world is arid or semi-arid, including much of the Polar Regions (including Third Pole). The area under study is a source of several rivers and the spatio-temporal changes of the palaeolakes that existed can address climate and tectonic understanding of the region. Being located in a cold arid desert, these lakes lack biotic proxies and in such cases grain-size distribution study can be used as one of the proxy indices to shed light on depositional conditions and thus past climatic variations. Thus, this paper addresses the sediment characteristics, behaviour and spatio-temporal variations within a single palaeo-lacustrine regime. The purpose of this study is to relate the lake level changes defined by abrupt changes in facies association in vertical sequences to the change in hydrological budget controlled by precipitation.

Geological setting and river system

The study area lies along the north-west/south-east trending Indus Suture Zone (ISZ), that

marks the collision of Indian and Eurasian plates during the Eocene (Searle, 1986) (Fig. 1A). Evolution of the Indus sedimentary basin in Ladakh along the ISZ from fore-arc basin to intermontane depression is characterized by a series of lithotectonic units representing marine to continental successions (Garzanti & Van Haver, 1988; Searle *et al.*, 1990; Sinclair & Jaffey, 2001; Clift, 2002). The region is bounded by the Zanskar Suture Zone to the south and the Shyok Suture Zone to the north (Thakur, 1981) (Fig. 1B). The rocks of the ISZ comprise (from north to south) the Ladakh magmatic arc, consisting of intrusives of the Ladakh plutonic complex, and the Indus sedimentary belt, referred to as the Indus Group/Indus Formation/Indus Molasse (consisting of conglomerate, sandstone, siltstone and shale) which rests directly on the Ladakh plutonic complex. South of the Indus Group, represented by Shergol and Nidar ophiolitic mélange, there are extrusives of the Dras and Khardung formations and flysch sediment of the Nidam and Lamayuru formations (Fig. 1B).

The ISZ dictates the course of the Indus River flowing through the region, originating on the Tibetan Plateau from the northern slope of Mount Kailas. It is one of the most important rivers of the Ladakh region and flows for a length of *ca* 500 km in India (mostly in the Ladakh region). On its way to the Arabian Sea it is joined by Shyok River, a major tributary, at Skardu on its right bank. On its left bank it is joined by Hanley River at Loma, with Zanskar, Yapola and Suru rivers forming few but major tributaries. Apart from the major tributaries, the Indus is also fed by numerous minor tributaries throughout its length on both of its banks. In the study area it is seen narrowing and meandering downstream and flowing through deep gorges (Fig. 1C).

STUDY AREA

Episodes of tectonic activity coupled with/without climatic perturbations during Late Quaternary and Holocene times were responsible for the

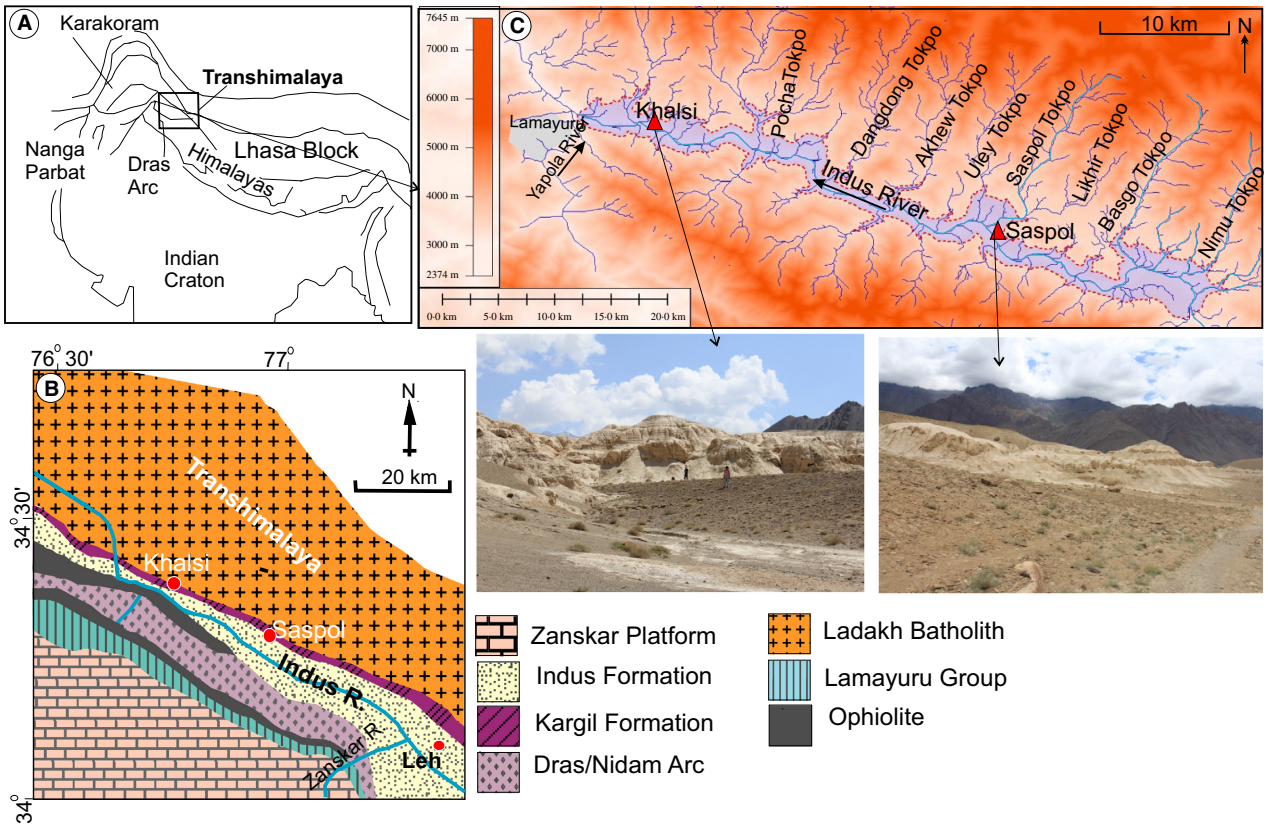

Fig. 1. (A) Location of the study area. (B) Geological map (modified after Clift, 2002). (C) Shuttle Radar Topographic Mission (SRTM) digital elevation model (DEM) of the study area showing the drainage pattern, extent of the palaeolake (dotted line), location of the Saspol and Khalsi palaeolake deposits with respect to the river system, and photographs of the Saspol and Khalsi palaeolake deposits.

damming of the Indus River and formation of barrier lakes. The two sedimentary sequences at Saspol (34°14.99′N, 77°10.94′E) and Khalsi (34°20.03′N, 76°52.54′E), which were part of the Saspol–Khalsi palaeolake reconstructed by Nag & Phartiyal (2015), were chosen for this study. These lakes are fed by meltwater from glaciers during warm climatic conditions and/or by precipitation during intensified monsoon phases. Both of the sections occur stratigraphically at almost the same elevation [Khalsi at 3285 m above the present day river level (aprl) and Saspol at 3268 m aprl on the right bank along the Indus River valley]. The Saspol section is *ca* 20 m thick and situated above Saspol Village *ca* 100 m aprl. At Khalsi village, two sets of fluvial terraces are recorded having an elevation difference of 100 m. The Khalsi palaeolake section (*ca* 18 m thick) is perched 50 m above the fluvial deposit consisting of sorted, stratified and rounded to sub-rounded gravels of the older terrace. The Saspol section is located upstream towards the centre of the lake, whereas the Khalsi section is situated close to the outlet near the blockage of the river (Fig. 1C). Two major tributaries, Saspol Nala and Likhir Nala, join the main river at Saspol on the right bank and the Yapola tributary joins the main trunk river at Khalsi on the left bank. The study area is the high-altitude region of Ladakh which is characterized by a cold, arid to semi-arid desert environment and is located in the vicinity of the tectonically active ISZ (Mohindra & Bagati, 1996; Kotlia & Rawat, 2004; Singh & Jain, 2007; Phartiyal & Sharma, 2009). The region endures severe climatic conditions defined by intensive weathering, frost action, extreme temperatures and tremendous erosion exacerbated by scant vegetation.

MATERIALS AND METHODS

Field work was carried out between Nimo and Khalsi, a stretch of *ca* 50 km that hosts several sedimentary facies types. A number of palaeolake sequences and associated fluvial and colluvial sediments were identified and mapped in the field with the help of Survey of India topographic maps and satellite data (Google Earth, ASTER-DEM). The height and location of lacustrine sections were taken from toposheets, altimeter and hand-held global positioning systems. The Saspol and Khalsi sections were taken as representative sections of the Saspol–Khalsi palaeolake system. The extent of the palaeolake was determined with the help of Global Mapper™ software with a basin fill model using the highest contour level of the sediment exposed as of today (Nag & Phartiyal, 2015). The exposed outcrops were scraped off to obtain fresh surfaces and systematic sampling was done without leaving any gap between consecutive samples for detailed sedimentological studies. Samples were properly labelled and extreme care was taken to avoid any kind of contamination.

Granulometric size analysis

The samples collected were unconsolidated in nature; they were gently pounded, soaked in distilled water overnight, air-dried, homogenized and chemically treated following Singh *et al.* (2015). Grain-size distributions of 165 samples from Saspol section (*ca* 20 m in thickness) and 115 samples from Khalsi section (*ca* 18 m in thickness) were determined with a laser particle size analyser Cilas 1190 (Cilas SA, Orléans, France) based on scattering of light through a given angle by particles of a given size. The Cilas 1190 instrument uses the volume of particles to measure their size in wet mode (using distilled water as a dispersing agent). About 100 mg of sample was introduced to obtain the grain-size data which measures grain sizes ranging from 0·04 to 2500 μm.

Statistical parameters

Grain-size data obtained were used to determine grain-size parameters using GRADISTAT software (Blott & Pye, 2001) which allows measurement by both the Folk & Ward (1957) and moments methods and also provides graphical representations. The present study uses logarithmic Folk & Ward formulae (based on a log normal distribution with ϕ size) and descriptions to calculate and define grain-size parameters, namely: mean grain size (Mz) measures the average size of the sediment; standard deviation (SD) measures the dispersion of the distribution around the mean and denotes the sorting of the sediment; skewness (SK) measures the symmetry of distribution around the mean; and kurtosis (KG) measures of the peakedness of the distribution.

This software also generates the frequency distribution curve representing the weight percentage of different fractions of sediments. The mean grain size is described using the Udden-Wentworth grade scale; SD, SK and KG are described using the scheme proposed by Folk & Ward (1957). The maximum, minimum and

average values of the parameters are given in Table 2 (Saspol section) and Table 3 (Khalsi section).

Scatter plots are derived from the statistical parameters by transferring the data into Microsoft Excel®. Bivariate plots of mean versus standard deviation, mean versus skewness and mean versus kurtosis have been constructed. These plots are useful in understanding the geological significance of the grain-size parameters with respect to the transporting medium, energy of depositing medium and conditions of deposition (Folk & Ward, 1957; Spencer, 1963; Sahu, 1964).

Chronology

Chronology for four samples (three from Khalsi and one from Saspol) has been used after Nag & Phartiyal (2015) and one sample from Saspol was dated by accelerator mass spectrometer (AMS) data of bulk sediment from Silesian University of Technology, Gliwice, Poland, and calibrated by IntCal09, atmospheric data from Reimer *et al.* (2009). Standard sample preparation method was adapted to make graphite targets which were analysed by mass accelerator along with primary and secondary standard and process blanks (Piotrowska, 2013). Details of the chronologies are given in Table 1.

RESULTS

Lithostratigraphy and grain-size parameters

Figure 1C shows the location of the two sections taken up for the study in reference to their position in the *ca* 55 km long lake that existed 14·6 ka. A detailed account of lithology for both Saspol and Khalsi sections has been done, and the stratigraphic description of sedimentary layers is achieved using grain-size data and other sedimentary characteristics.

Saspol section

According to grain size, colour variation and lithofacies the palaeolake sequence is divided into 12 units (Unit S1 to Unit S12). For each unit mean (Mz), standard deviation (SD), skewness (SK) and kurtosis (KG) has been calculated. Sand, silt and clay percentages are calculated for each unit and shown in (Fig. 2).

Unit S1: Silty sand bed

This unit consists of *ca* 1·2 m thick, massive and dark greyish very coarse silt and medium to fine sand. Unit S1 consists of six samples and is a polymodal mixture of medium to very fine sand and very coarse to coarse silt. The samples are poorly sorted with fine to very fine skewness and mesokurtic to leptokurtic grain-size distribution.

Unit S2: Alternate fine silt and clay bed

This unit consists of *ca* 0·4 m thick alternating bands of dark greyish fine silt and yellowish clay. The bands are a few centimetres in scale; however, they are not of uniform thickness. Unit S2 consists of four samples. The samples are polymodal in nature and consist of poorly sorted fine silt and clay. Fine to very fine silt sediments show fine skewness while clay shows a coarse skewed value and platykurtic to mesokurtic grain-size distribution.

Table 1. Accelerator mass spectrometer (AMS) radiocarbon chronology of the Saspol and Khalsi sections (Ages 1, 3, 4 and 5 are taken from Nag & Phartiyal (2015).

SN	Sample name	Locality	Lab. no.	Age ^{14}C (BP)	Calendar age (calibrated) – 68% intervals	Calendar age (calibrated) – 95% intervals
1	LS-88	Saspol	GdA-3110	10 850 ± 45	12 755 BP (68·2%) 12 701 BP	12 800 BP (95·4%) 12 687 BP
2	LS-268	Saspol	GdA-4255	7871 ± 38	8715 BP (68·2%) 8596 BP	8780 BP (90·9%) 8557 BP
3	KI-153	Khalsi	GdA-3271	11 020 ± 55	12 973 BP (68·2%) 12 805 BP	13 029 BP (95·4%) 12 739 BP
4	KI-175	Khalsi	GdA-3283	9715 ± 265	11 599 BP (2·6%) 11 553 BP 11 477 BP (2·3%) 11 435 BP 11 409 BP (63·2%) 10 659 BP 10 613 BP (0·2%) 10 609 BP	12 029 BP (95·1%) 10 375 BP 10 320 BP (0·3%) 10 300 BP
5	KI-230	Khalsi	GdA-3557	5175 ± 30	5984 BP (12·7%) 5973 BP 5943 BP (55·5%) 5910 BP	5991 BP (95·4%) 5902 BP

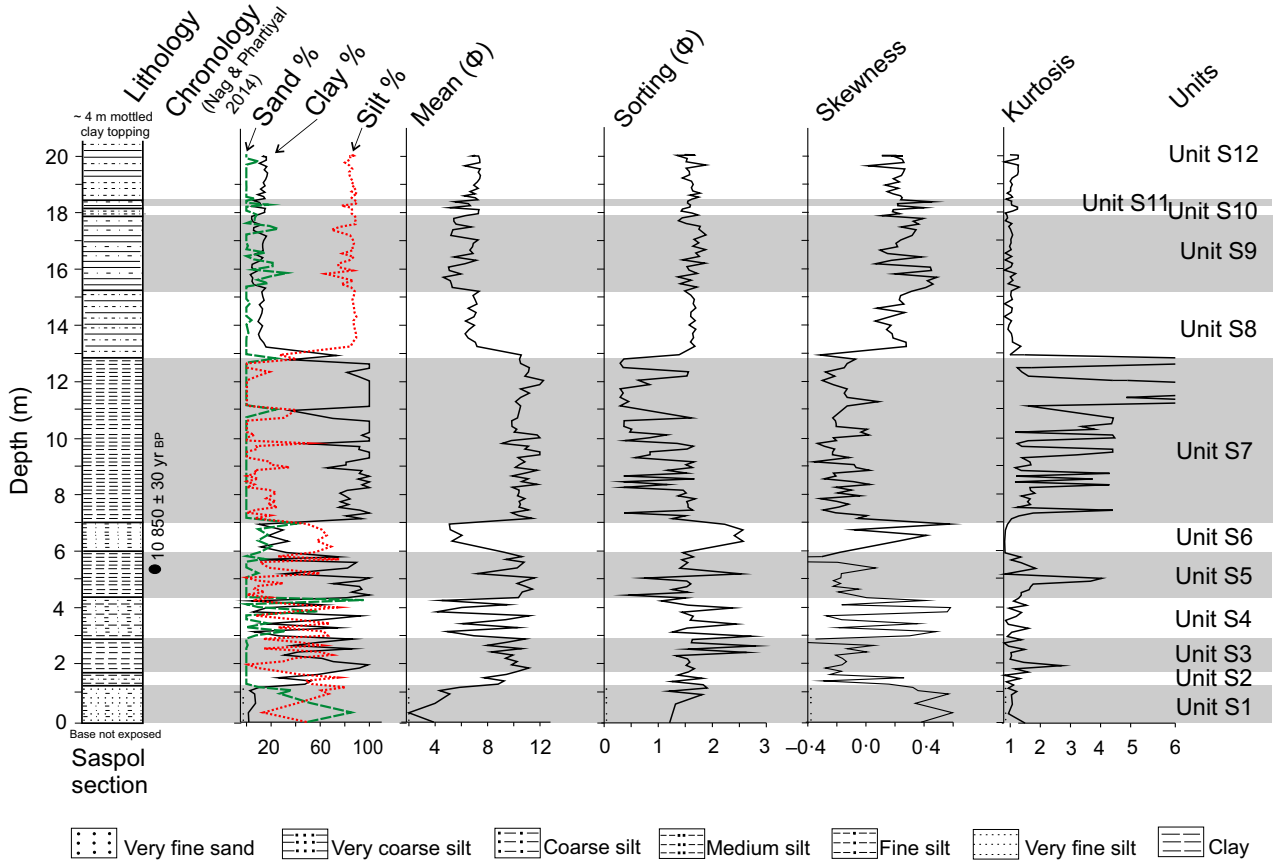

Fig. 2. Lithology of the Saspol palaeolake sequence with AMS radiocarbon chronology (Nag & Phartiyal, 2015) showing Sand, Silt and Clay percentages, along with Mean, Standard Deviation, Skewness and Kurtosis variations with depth of the Saspol section.

Unit S3: Massive clay bed

This unit is represented by *ca* 1·4 m of yellowish massive clay. Unit S3 consists of 11 samples. These samples are mostly polymodal, only 9% of samples are bimodal, poorly sorted clay sediments with a coarse skewed and mesokurtic to very leptokurtic grain-size distribution.

Unit S4: Inter-layered silt and clay bed

This unit is comprised of *ca* 1·3 m thick interlayered very coarse to medium silt and clay. The layers are a few centimetres in scale and of unequal thickness. Unit S4 consists of 10 samples, polymodal, very poorly to poorly sorted, very coarse to medium silt and clay. Skewness ranges from coarse skewed (for clay) to symmetrical to fine skewed (for silt) and mesokurtic to very leptokurtic grain-size distribution; 20% of the samples show platykurtic distribution.

Unit S5: Bedded clay bed

This unit consists of a *ca* 1·7 m thick yellowish clay bed and contains reddish clay bands in places. Unit S5 consists of 14 samples; 64% of the samples show bimodal distribution and 34% are polymodal in nature. Samples are moderately to poorly sorted clay with a symmetrical to coarse skewed and leptokurtic to very leptokurtic grain-size distribution.

Unit S6: Coarse to medium silt bed

This unit is a *ca* 1 m thick massive greyish coarse silt bed. Unit S6 consists of four samples, polymodal, very poorly sorted coarse to medium silt with a symmetrical to very fine skewed and platykurtic to mesokurtic grain-size distribution.

Unit S7: Massive clay bed

This unit is *ca* 6 m thick and consists of a massive yellowish clay bed. Unit S7 consists of 48 samples. Most of the samples are trimodal to

bimodal in nature. Some samples are unimodal (16%) well to very well-sorted clay. Samples exhibit a symmetrical to negatively skewed and mesokurtic to extremely leptokurtic grain-size distribution.

Unit S8: Inter-layered medium and fine silt bed

This unit consists of *ca* 2 m of inter-layered medium and fine silt. Mean grain size of medium silt decreases (6·2 to 6·8 ϕ) towards the top. Unit S8 consists of 14 samples and represents polymodal, poorly sorted, medium to fine silt with a symmetrical to fine skewed and platykurtic to mesokurtic grain-size distribution.

Unit S9: Coarse to medium silt bed

This unit is *ca* 3 m thick and consists of massive coarse to medium silt, comprising 22 samples which are polymodal, poorly sorted very coarse to medium silt with a very fine to fine skewness and platykurtic to mesokurtic grain-size distribution.

Unit S10: Fine silt bed

This unit is made up of fine silt beds *ca* 0·2 m thick and consists of three samples. Sediments are polymodal, poorly sorted fine silt with a fine skewed and platykurtic to mesokurtic grain-size distribution.

Unit S11: Coarse to medium silt bed

This unit consists of greyish coarse to medium silt of *ca* 0·3 m thickness. Four samples of this unit show polymodal, poorly sorted coarse to medium silt with a very fine to fine skewed and mesokurtic to leptokurtic grain-size distribution.

Unit S12: Fine silt bed with medium silt intercalations

This unit is a *ca* 1·6 m thick fine silt bed intercalated occasionally with medium silt of millimetre-scale thickness. This unit consists of 19 samples, polymodal, poorly sorted medium to fine silt with a fine skewed and platykurtic to leptokurtic grain-size distribution.

Bivariate plots for Saspol section

Mean size (Mz) versus Standard Deviation (SD): Figure 3A shows that samples from Saspol section ranged from well-sorted to very poorly sorted sediments.

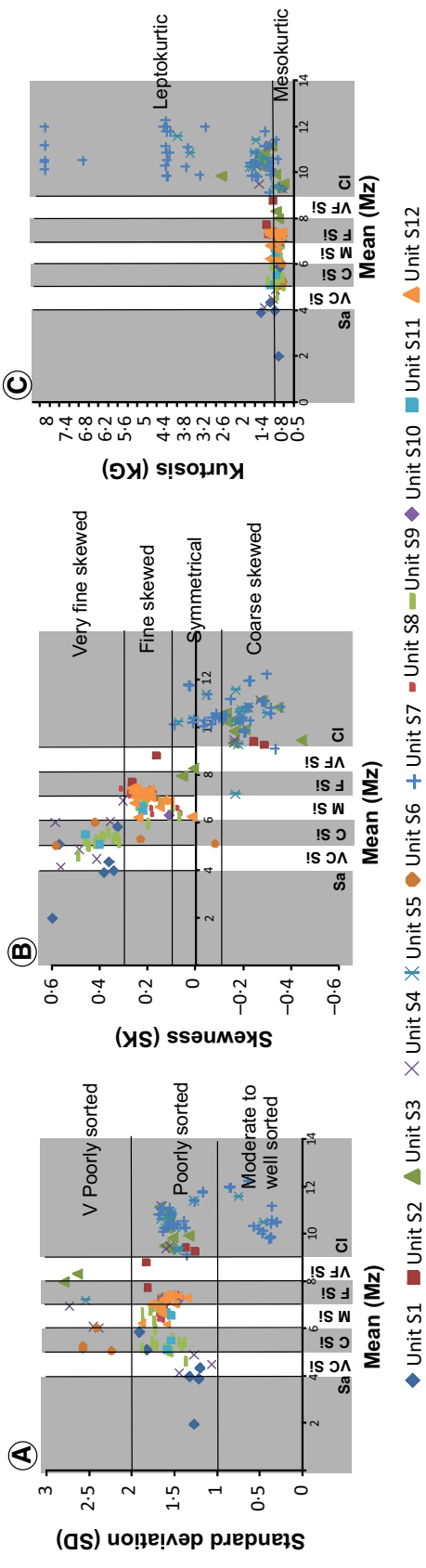

Fig. 3. (A) Bivariate plot of standard deviation (σ) versus mean size (Mz) for each unit of a 20 m thick Saspol palaeolake section. (B) Bivariate plot of Skewness (SK) versus mean size (Mz) for each unit of the Saspol section. (C) Bivariate plot of Kurtosis (KG) versus mean size (Mz) for each unit of the Saspol section.

• Mean size ranging from 1·99 to 5·85 ϕ (sand dominant) for Unit S1, the SD value varies between 1·19 ϕ and 1·9 ϕ.
• For mean grain-size values from 4·41 to 8·81 ϕ (silt dominant) of Units S2, S4, S6 and Units S8 to S12, SD ranged between 1·05 ϕ and 2·72 ϕ.
• Mean size of more than 9 ϕ (clay dominant) (Units S3, S5 and S7) have SD values between 0·29 ϕ and 2·6 ϕ.

The plot demonstrates a trend that the degree of sorting decreases as mean grain size shifts from sand to silt. The SD value then increases again as the grain size shifts to the clay sediments. Sorting is poorest (SD value maximum) in coarse to fine silt. Only the clay size fraction of Unit S7 shows well-sorted sediments.

Mean size (Mz) and Skewness (SK): Figure 3B shows that skewness is the function of mean size. From the plot it is seen that coarse-grained sediment including sand to coarse silt exhibit very fine (positive) skewness. With a decrease in grain size from medium to fine silt the value of skewness decreases. Skewness becomes coarse (negative) with a further decrease in grain size to clay.

• Unit S1 (Mz – 1·99 to 5·85 ϕ), Unit S6 (Mz – 5·07 to 6·04 ϕ), Unit S9 (Mz – 4·62 to 7·27 ϕ) and Unit S11 (Mz – 5·11 to 6·68 ϕ) (sand to coarse slit dominant) is very finely skewed, with values ranging more than 0·3.
• Value of skewness decreases with the decrease of mean size, i.e. in the range of medium to fine silt. In Unit S8 (Mz – 6·28 to 7·35 ϕ), Unit S10 (Mz – 7·30 to 7·35 ϕ) and Unit S12 (Mz – 6·21 to 7·45 ϕ) (medium to fine silt dominant) the value of skewness ranged from 0·1 to 0·3.
• The mean grain size belonging to the clay fraction, i.e. more than 9 ϕ (Units S3, S5 and S7) shows a symmetrical to coarse (negative) skewed distribution.

Thus, overall the value of skewness tends to decrease as the sediments change from a coarser to a finer size.

Mean size (Mz) versus Kurtosis (KG): Figure 3C shows that the end members (sand and clay) depict high kurtosis values while the silt mode shows kurtosis ranging from mesokurtic to leptokurtic distribution.

• Unit S1 (sand dominant) and Units S3, S5 and S7 (clay dominant), show a range of kurtosis values from 0·94 to 8·12. These units indicate that the majority of the samples are leptokurtic to extremely leptokurtic and a few of them show a mesokurtic distribution. Unit S7 has the maximum KG value of 8·12.
• Units S2, S4, S8, S9, S11 and S12 (silt dominant) exhibit a mesokurtic distribution for the majority of the sediments and some show leptokurtic distribution. The points are clustered around a kurtosis value of 0·9 to 1·1.
• The platykurtic nature of units S6 and S10 depicts a sub-equal proportion of different modes occurring together.

Khalsi section

The Khalsi palaeolake section is more than 18 m thick and located at an altitude of 3250 m (Fig. 1C). The section is exposed above Khalsi village at *ca* 100 m aprl. Based on grain size, lithofacies and colour variation the entire section is divided into 13 units (Unit K1 to Unit K13; Figs 4 and 5). Sand, silt and clay percentages for each unit are calculated and shown in Fig. 4.

Unit K1: Coarse to fine silt with very coarse silty partings
This unit is *ca* 1·4 m thick and consists of a greyish medium to fine silty bed. At two intervals the bed is punctuated by millimetre-scale thick very coarse silty partings. Unit K1 consists of 13 samples which are polymodal, poorly sorted very coarse to fine silt with a very fine to fine skewed and mesokurtic to leptokurtic grain-size distribution.

Unit K2: Very fine sand bed
This unit is *ca* 1·6 m thick and consists of massive, greyish very fine sand deposits. This facies has a gradational contact with the underlying unit. Unit K2 consists of five samples which are polymodal, moderately to poorly sorted very fine sand with very fine skewness values and a very leptokurtic grain-size distribution.

Unit K3: Laminated medium to fine silt bed
This unit consists of *ca* 1 m thick laminated fine silt sediments. The laminae are a few centimetres thick. Fine silt is inter-layered with medium silt at a few locations. Unit K3 consists of eight samples. Samples are polymodal, poorly sorted medium to fine silt with a fine skewed and leptokurtic grain-size distribution.

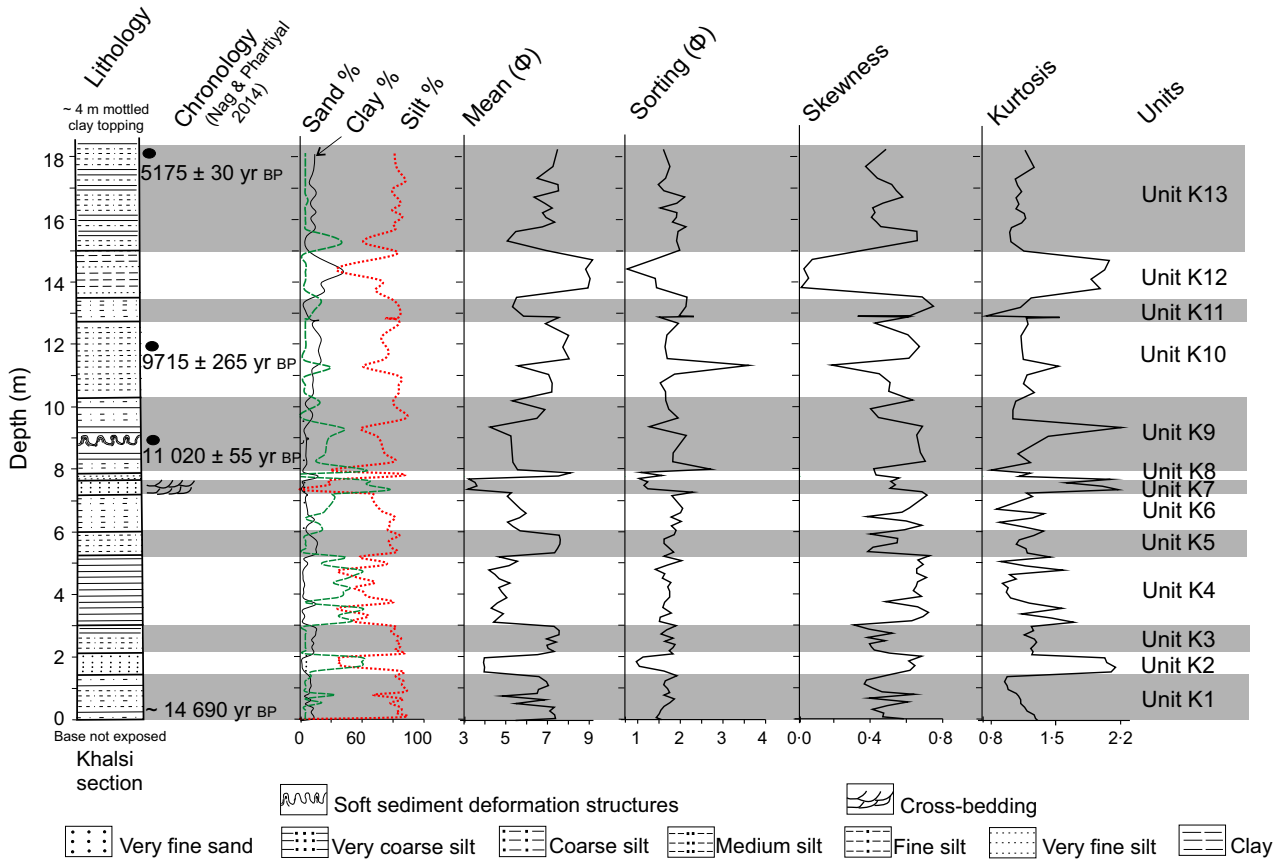

Fig. 4. Lithology of the Khalsi palaeolake sequence with AMS radiocarbon chronology (Nag & Phartiyal, 2015) showing Sand, Silt and Clay percentages, along with mean, standard deviation, skewness and kurtosis variations with depth of the Khalsi section.

Unit K4: Very coarse silt bed
This unit is *ca* 2·2 m thick massive greyish very coarse silt. Unit K4 consists of 15 samples, polymodal, poorly sorted very coarse and coarse silt with a very fine skewed and mesokurtic to very leptokurtic grain-size distribution.

Unit K5: Fine silt bed
This unit is composed of fine silt sediment *ca* 0·7 m thick. Unit K5 consists of five samples, polymodal, poorly sorted fine silt showing a fine skewed and mesokurtic to leptokurtic grain-size distribution.

Unit K6: Coarse silt bed
This unit is *ca* 1·2 m thick and consists of greyish massive coarse silt deposits. Unit K6 consists of eight samples, polymodal, very poorly to poorly sorted coarse to medium silt with a very fine to fine skewed and platykurtic and leptokurtic grain-size distribution.

Unit K7: Small-scale cross-bedded very fine sand bed
This unit is *ca* 0·5 m thick and made up of very fine sand showing small-scale low angle cross-bedding. Unit K7 consists of four samples. Samples are polymodal, poorly sorted very fine sand with a very fine skewed and very leptokurtic grain-size distribution.

Unit K8: Very fine silt bed
This unit is 10 cm thick very fine silt and consists of two samples, polymodal, very poorly to poorly sorted fine to very fine silt with a very fine skewness value and mesokurtic to leptokurtic grain-size distribution.

Unit K9: Coarse to medium silt bed
This unit is comprised of a *ca* 2 m thick massive silty bed. At the 8·7 m interval, this unit shows a deformation level consisting of (Figs 3 and 5B) convolute and pseudonodule

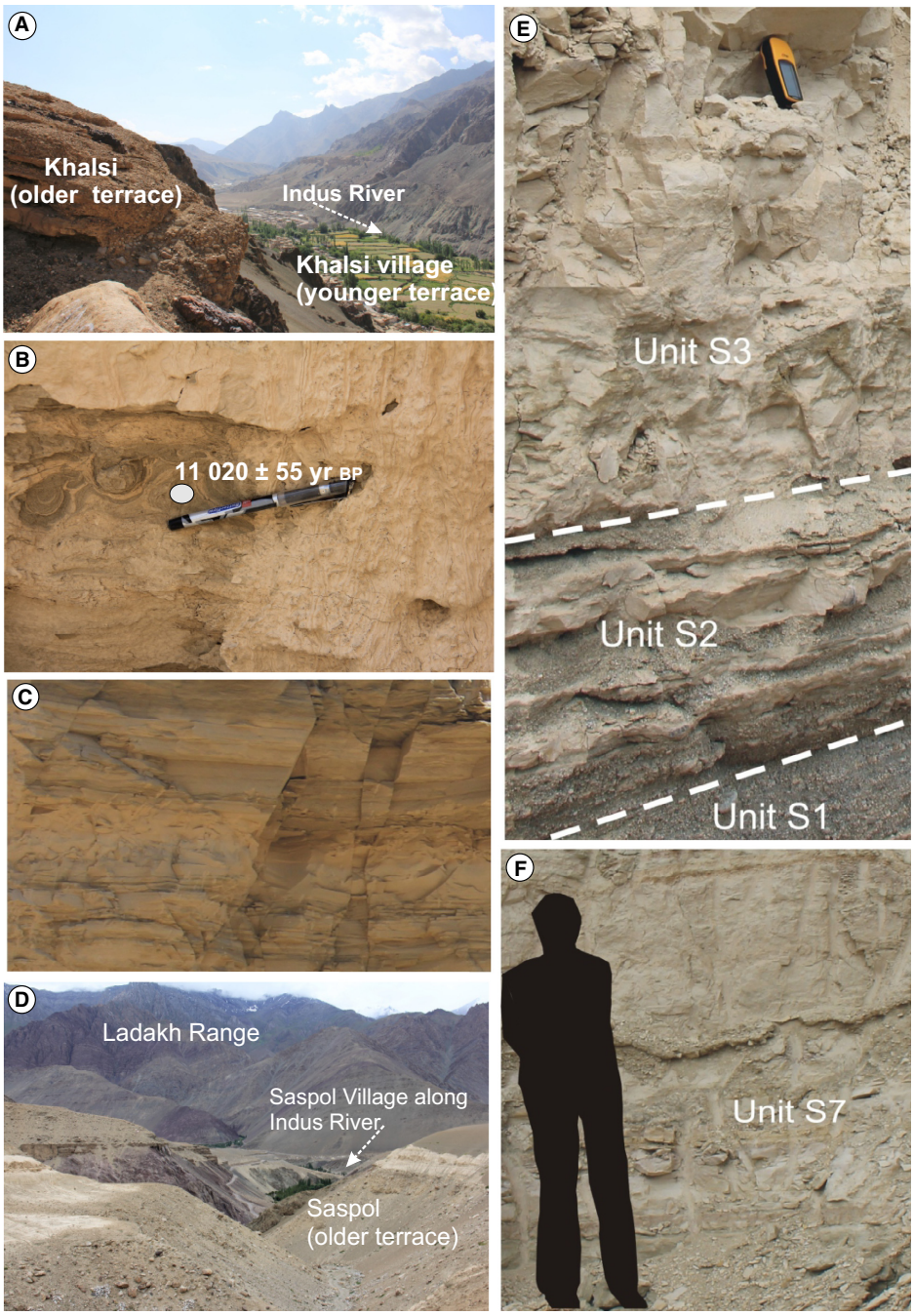

Fig. 5. (A) Photographs showing two sets of fluvial terraces at Khalsi village. The Khalsi palaeolake deposit is perched on the older terrace. (B) Soft deformation layer in Khalsi section at 3287 m dated to 11 020 ± 55 yr BP. Pen for scale is 15 cm long. (C) Unit K12 (1·2 m) of Khalsi section showing greyish yellow silty clay deposit. (D) Saspol palaeolake deposits perched on the older fluvial terrace at the 3268 m level. (E) Photograph showing Units S1 to S3 of the Saspol section; the silty sand bed of Unit S1 indicating fluvial activity. Alternate silt and clay bed of Unit S2 overlain by massive clay (Unit S3). GPS unit for scale is 11 cm long. (F) Massive clay bed representing Unit S7 of the Saspol section showing the most stable lake phase. Person for scale is ca 1.6 m tall.

structures. This bed is dated to 11 020 ± 55 year BP (Nag & Phartiyal, 2015). Eight samples are polymodal, very poorly to poorly sorted coarse to medium silt with a very fine to fine skewed and mesokutic to leptokurtic grain-size distribution.

Unit K10: Fine silt bed
This unit consists of fine silt facies *ca* 3 m thick. Ten samples are analysed which show polymodal, poorly sorted fine to very fine silt with a fine to very fine skewed and leptokurtic to very leptokurtic grain-size distribution.

Unit K11: Coarse silt bed
This unit is represented by 0·6 m of coarse silt and consists of three samples which are trimodal, poorly to very poorly sorted with a very fine skewed and leptokurtic grain-size distribution.

Unit K12: Very fine silt and clay facies
This unit consists of *ca* 1·2 m thick greyish yellow massive silty clay. Four samples of the facies analysed showed a bimodal sediment nature, moderately to poorly sorted very fine silt and clay with a coarse skewed and very leptokurtic grain-size distribution.

Unit K13: Coarse to fine silt bed
This unit is a *ca* 3 m greyish silty bed and consists of 15 samples. Sediments are polymodal, very poorly to poorly sorted coarse to fine silt with a very fine to fine skewness and mesokurtic to leptokurtic grain-size distribution.

Field photographs of both the Saspol and Khalsi sections are shown in Fig. 5.

Bivariate plots for Khalsi section

Mean size (Mz) versus Standard Deviation (SD): Figure 6A shows that the samples are overall poorly sorted. From the plot, a trend similar to that of Saspol is seen. The degree of sorting decreases as mean grain size shifts from sand to silt. Sorting increases as the grain size shifts to the clay sediments.

- Units K2 and K7 (Mz – 3·17 to 3·98 ϕ) representing very fine sand show a SD value ranging from 0·96 to 1·61 ϕ.
- Sorting decreases, i.e. the SD value increases ranging from 1·41 to 2·29 ϕ as the size decreases in units K4, K6 and K11, representing very coarse to medium silt (Mz – 4·18 to 5·97 ϕ).
- In Units K1, K3, K5, K8, K9, K10 and K13 (medium to fine silt) the SD value decreases (from 1·07 to 3·6 ϕ).
- Very fine silt to clay samples of Unit K12 (Mz – 8·9 to 9·1 ϕ) shows better sorting and the SD varies from 0·75 to 1·44 ϕ.

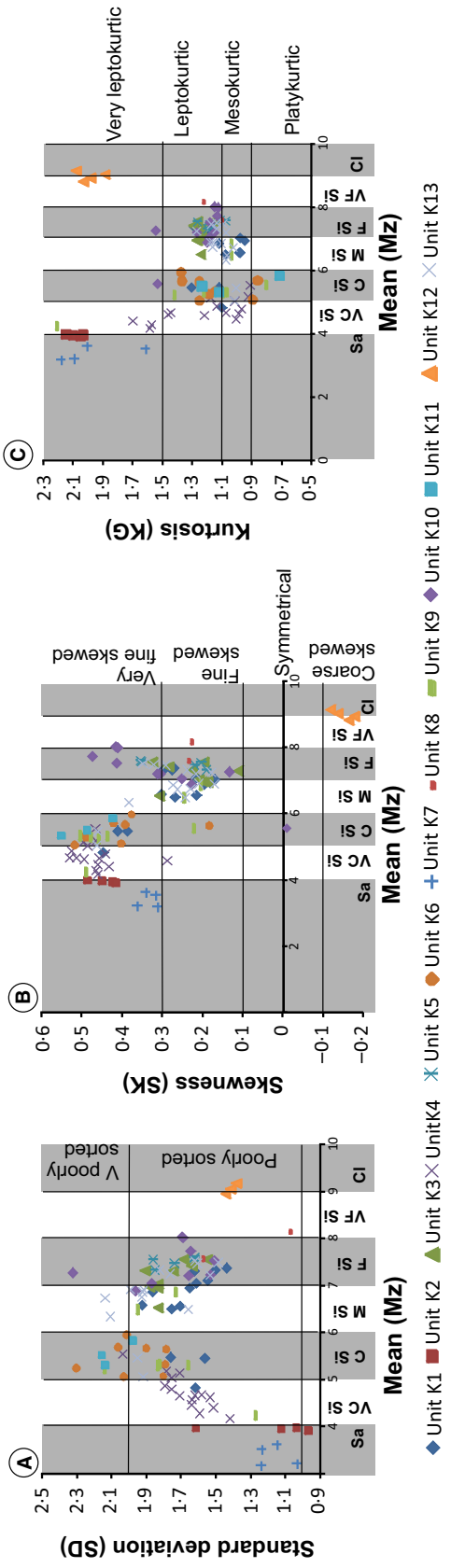

Fig. 6. (A) Bivariate plot of standard deviation (SD) versus Mean size (Mz) for each unit of the Khalsi palaeolake section. (B) Bivariate plot of Skewness (SK) versus mean size (Mz) for each unit of the Khalsi section. (C) Bivariate plot of Kurtosis (KG) versus mean size (Mz) for each unit of the Khalsi section.

Mean size (Mz) versus Skewness (SK): Figure 6B shows that fine (positive) skewness is attained by sand to coarse silt sediment and decreases with a decrease in grain size.

- Units K2, K4, K6, K7 and K11 display a very fine (positive) skewed grain-size distribution (0·37 to 0·54). The mean size of the sediments for these units ranges from very fine sand to coarse silt (3·17 to 5·97 ϕ).
- For Units K3, K5, K8 and K10 (Mz – 6·90 to 8·10 ϕ, medium to very fine silt) the value of skewness decreases varying from −0·01 to 0·47. However, Units K1, K9 and K13 have a wide range of grain sizes and show a very fine to fine skewed distribution.
- Unit K12 (mean size ranging from 8·8 to 9·1 ϕ, clay dominant) shows a coarse (negative) skewed grain-size distribution.

Mean (Mz) versus Kurtosis (KG): Figure 6C shows that most of the samples have a leptokurtic distribution for sand and clay sediments. The mean size range represented by Units K2 and K7 (Mz – 3·1 to 3·9 ϕ) consisting of medium to fine sand and Unit K12 (Mz – 8·8 to 9·1 ϕ) consisting of very fine silt to clay display a very leptokurtic (1·8 to 2·17) distribution. The rest of the units, consisting dominantly of silt, display a mesokurtic to leptokurtic distribution from 0·9 to 1·69. Only 3% of the samples show a platykurtic distribution.

Frequency distribution curve

The frequency distribution curve shows the weight percentage of different sediment fractions. Figure 7A and B shows polymodal distribution of sediments in the Saspol and Khalsi sections, respectively. The polymodal nature arises from the mixture of sand, silt and clay components within a single grain-size distribution. In Unit S7 of Saspol, 16% of the sample shows unimodal distribution.

DISCUSSION

The Indus River, the backbone of Ladakh flows for a length of 422 km in India with a basin area of 25 607 km^2. The river width is very narrow (less than a kilometre) and strictly follows the Indus Suture Zone (ISZ) in the study area. Large-scale sediments from the barren steep mountain slopes, along both banks of the river tend to mobilize during intensified monsoon phases and tectonic events which generate rock avalanches and landslides. The huge amount of debris thus produced by such events has the potential to dam the drainage at constricted places forming lakes, and later breaching of such lakes results in catastrophic flooding downstream. These phenomena are common occurrences and have been documented several times along the Indus River valley (Mason, 1929; Hewitt, 1982; Burbank, 1983; Phartiyal *et al.*, 2005; Phartiyal & Sharma, 2009). During the last 40 ka, the Indus River has been dammed several times and four phases of lake formation are recorded till date, at: *ca* 35 to 26 ka (Lamayuru palaeolake); 17 to 13 ka (Rizong palaeolake); 14 to 5 ka (Saspol–Khalsi palaeolake); and 10 to *ca* 1·5 ka (Spituk–Leh palaeolake) (Phartiyal *et al.*, 2013; Nag & Phartiyal, 2015). Breaching of Lamayuru palaeolake (aerial extent 3·524 km^2) along the Yapola River (a tributary of the Indus) at the closure of the last glacial maximum (LGM; Fort *et al.*, 1989; Kotlia *et al.*, 1997a,b, 1998; Nag & Phartiyal, 2015) generated a huge amount of debris which choked the Indus River channel near Mizdo (downstream of Khalsi; Fig. 1C) leading to a rise of water level upstream. Gradually the water from the main channel and contributions from tributaries caused the water level to rise further to a level of more than 3200 m; this led to the formation of a *ca* 55 km long lake extending from Nimo to Khalsi, having a surface area of 370 km^2. Two sections representing the lake – Saspol and Khalsi, separated by a distance of 35 km – were selected based on their position within the lake system to carry out the grain-size distribution studies. The variations in sediment character of both sections of the Saspol–Khalsi palaeolake in the same chronological framework are shown in Fig. 8. Tables 2 and 3 present the overall sediment character of each unit for both sections.

In this study sediment texture, as defined by grain-size parameters, shows that sediment composition in both of the sections is controlled by the mixing of three grain-size populations – sand, silt and clay. Inter-relation of the statistical parameters is used to give an insight into the depositional energy conditions. Mean size measures the average size of the sediment, thus indicating the overall energy condition of the depositing medium (Folk & Ward, 1957; Folk, 1966). Several studies on grain-size distribution

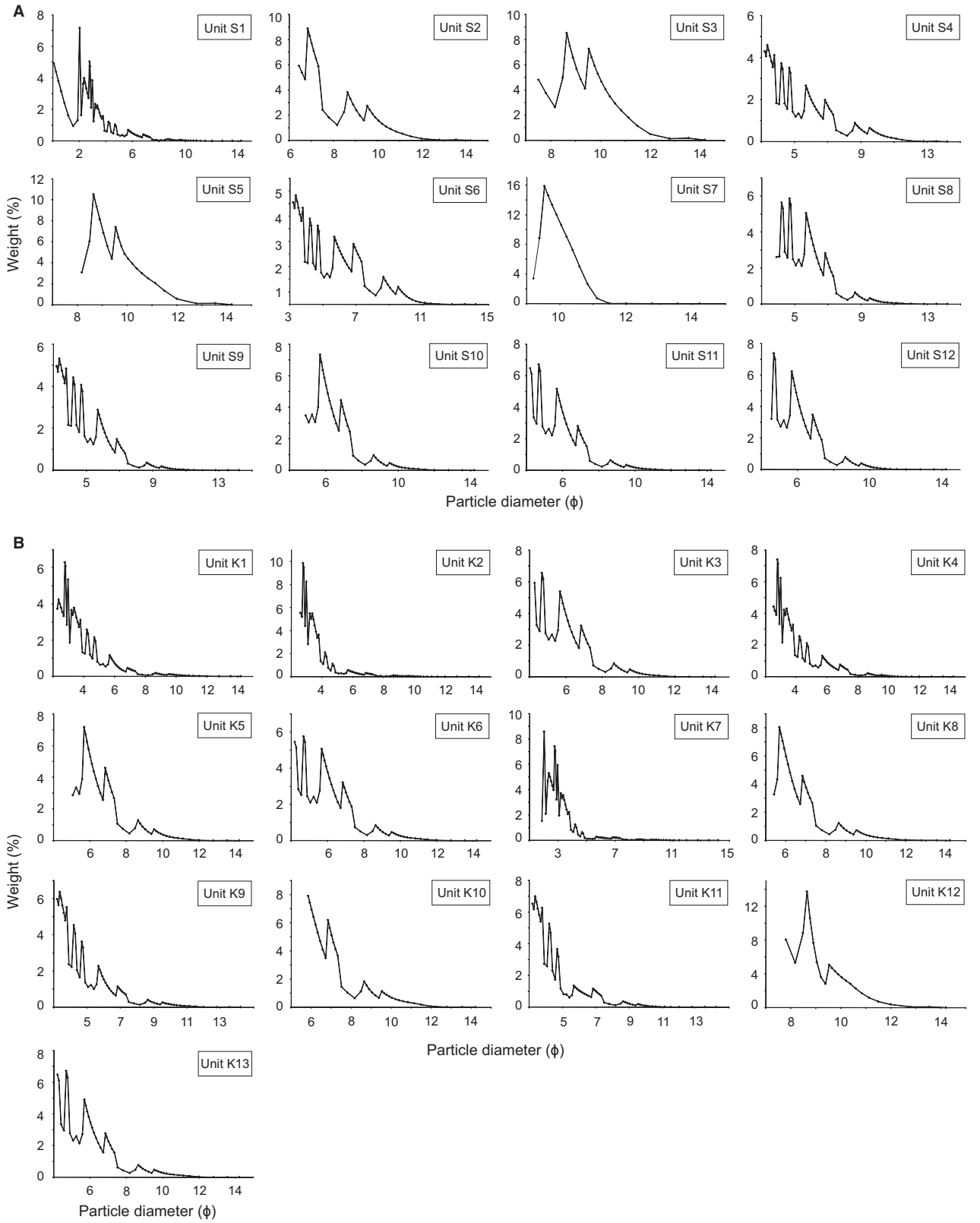

Fig. 7. (A) Representative frequency distribution curves for each unit of the Saspol section showing a polymodal grain-size distribution. (B) Representative frequency distribution curves for each unit of the Khalsi section showing a polymodal grain-size distribution.

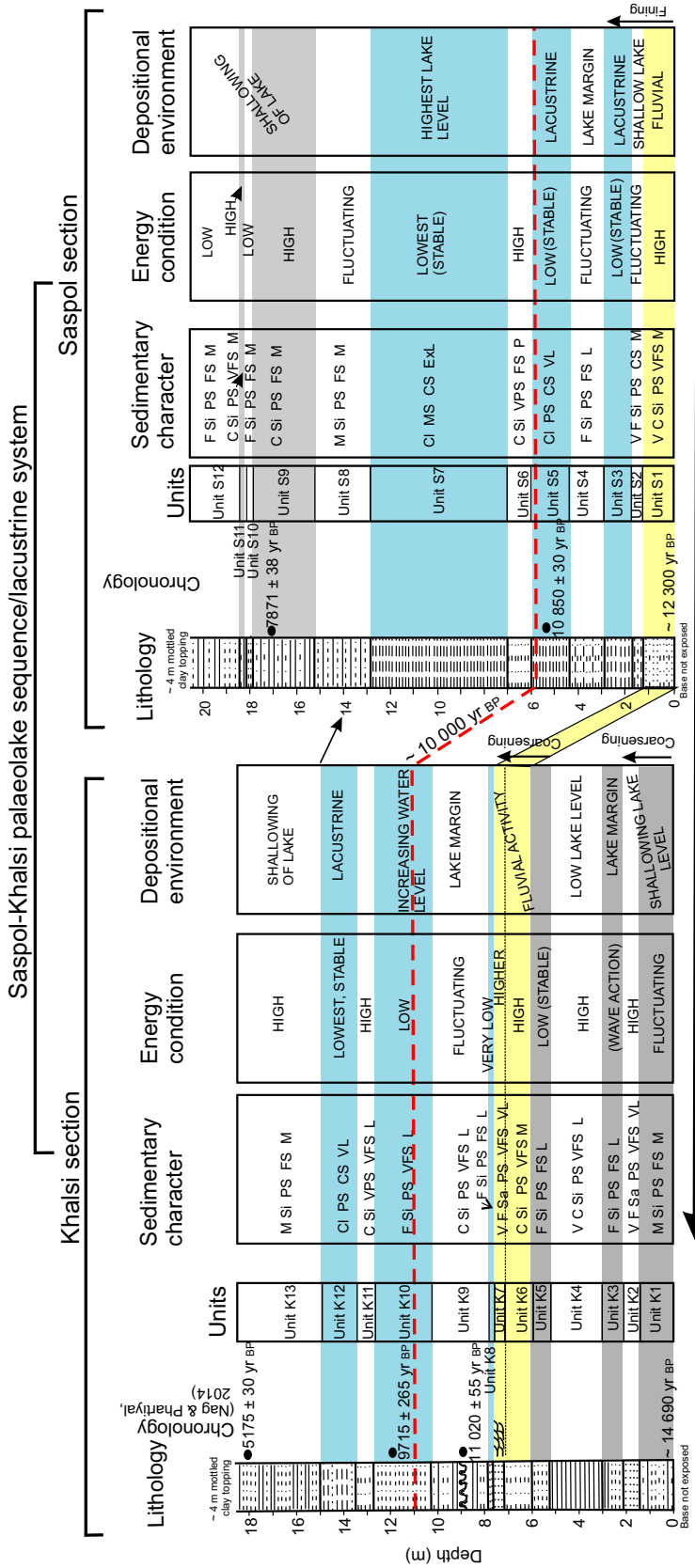

Fig. 8. Comparison of the sedimentary character, energy condition and depositional environment of the two sections (Saspol and Khalsi) of a single valley lake system (Sa, Sand; V C Si, very coarse silt; C Si, coarse silt; M Si, medium silt; F Si, fine silt; V F Si, very fine silt; Cl, clay; MS, moderately well-sorted; PS, poorly sorted; VPS, very poorly sorted; VFS, very fine skewed; FS, fine skewed; CS, coarse skewed; P, platykurtic; M, mesokurtic; L, leptokurtic, VL, very leptokurtic, ExL, extremely leptokurtic).

Table 2. Statistical measures of grain-size distributions of the Saspol Palaeolake section.

Units		Mean ϕ	Standard deviation ϕ	Skewness	Kurtosis
S1:	Max	5·85	1·90	0·38	1·49
	Min	1·99	1·19	0·32	0·93
	Average	4·19	1·45	0·36	1·11
S2:	Max	9·43	1·83	0·26	1·31
	Min	7·73	1·25	−0·29	0·80
	Average	8·81	1·56	−0·02	1·02
S3:	Max	11·15	2·79	0·05	2·70
	Min	7·96	1·32	−0·55	0·79
	Average	9·83	1·76	−0·17	1·32
S4:	Max	11·19	2·72	0·58	1·60
	Min	4·14	1·05	−0·27	0·84
	Average	7·30	1·76	0·18	1·15
S5:	Max	11·59	1·50	0·06	4·04
	Min	7·21	0·45	−1·78	0·81
	Average	10·29	1·44	−0·26	1·71
S6:	Max	6·04	2·56	0·57	0·90
	Min	5·07	2·23	−0·08	0·81
	Average	5·39	2·44	0·28	0·84
S7:	Max	12·26	1·68	0·08	8·12
	Min	9·12	0·29	−0·35	0·98
	Average	10·69	0·98	−0·16	3·12
S8:	Max	7·35	1·69	0·31	1·35
	Min	6·28	1·48	0·06	0·80
	Average	6·86	1·63	0·20	1·02
S9:	Max	7·27	1·88	0·48	1·29
	Min	4·62	1·36	0·06	0·80
	Average	5·90	1·64	0·29	0·99
S10:	Max	7·35	1·62	0·23	0·83
	Min	7·3	1·42	0·18	1·23
	Average	7·31	1·49	0·20	1·04
S11:	Max	6·68	1·59	0·21	1·24
	Min	5·11	1·54	0·45	1·03
	Average	5·96	1·56	0·32	1·09
S12:	Max	7·45	1·88	0·26	1·27
	Min	6·21	1·34	0·01	0·80
	Average	7·07	1·60	0·20	1·08

Table 3. Statistical measures of grain-size distributions of the Khalsi Palaeolake section.

Units		Mean ϕ	Standard deviation ϕ	Skewness	Kurtosis
K1:	Max	7·38	1·92	0·44	1·30
	Min	4·82	1·43	0·16	0·94
	Average	6·57	1·65	0·27	1·11
K2:	Max	3·98	1·61	0·48	2·14
	Min	3·93	0·96	0·41	2·02
	Average	3·96	1·18	0·44	2·08
K3:	Max	7·55	1·90	0·32	1·29
	Min	6·52	1·54	0·11	1·15
	Average	7·18	1·76	0·22	1·24
K4:	Max	5·55	2·03	0·52	1·69
	Min	4·18	1·41	0·28	0·90
	Average	4·75	1·66	0·46	1·20
K5:	Max	7·61	1·84	0·35	1·26
	Min	7·34	1·61	0·18	1·07
	Average	7·51	1·73	0·26	1·16
K6:	Max	5·97	2·29	0·51	1·37
	Min	5·08	1·78	0·18	0·85
	Average	5·47	1·95	0·40	1·16
K7:	Max	3·62	1·23	0·36	2·17
	Min	3·17	1·14	0·31	1·61
	Average	3·38	1·16	0·33	1·96
K8:	Max	8·10	1·57	0·23	1·20
	Min	7·52	1·07	0·22	1·10
	Average	7·81	1·32	0·22	1·16
K9:	Max	6·87	2·71	0·50	2·21
	Min	4·24	1·27	0·20	0·80
	Average	5·54	1·89	0·37	1·23
K10:	Max	8·03	3·60	0·47	1·54
	Min	6·90	1·50	−0·01	1·12
	Average	7·25	1·94	0·29	1·24
K11:	Max	5·85	2·15	0·54	1·23
	Min	5·32	1·97	0·42	0·70
	Average	5·56	2·08	0·48	1·01
K12:	Max	9·16	1·44	−0·11	2·07
	Min	8·82	0·75	−0·18	1·88
	Average	8·99	1·24	−0·15	1·99
K13:	Max	7·52	2·13	0·46	1·26
	Min	5·07	1·48	0·16	1·00
	Average	6·80	1·81	0·28	1·10

of lakes (Thomas *et al.*, 1972, 1976; Sly, 1978; Håkanson & Jansson, 1983; Peng*et al.*, 2005; Xiao *et al.*, 2009) show a direct correlation between the clastic deposits of lakes and a hydraulic energy regime; fine-grained deposits in the offshore regions are related to decreasing hydraulic energy and coarse-grained deposits are related to high energy conditions. The Saspol–Khalsi palaeolake, being a valley lake and bounded by steep mountain walls, cannot expand much laterally. Current and wave motion form the prime energy controlling the mean grain size and sediment sorting. The sediment composition of the lake is thus a function of water depth. The mean size representing clay deposits (Units S3, S5, S7 of Saspol section and Unit K12 of Khalsi section) is assigned to the

increasing water level and lowest energy condition, whereas a drop in water level causes erosion of the exposed shoreline and deposition of coarse-grained sediment (sand to coarse silt) representing a high energy nearshore environment. The SD represents fluctuations in the kinetic energy or velocity conditions of the depositing agent (Folk & Ward, 1957; Folk, 1974) and has an inverse relation with sorting of the sediment. The Mz versus SD plots (Figs 5A and 6A) show that SD increases as sediment size shifts from sand to silt and then decreases as sediment reaches clay size. Thus, the poorest sorting is exhibited by grain sizes ranging from coarse to fine silt. This trend is seen in both of the sedimentary sequences. The poorly sorted nature of the deposit is seen for both sections, except for Unit S7 of Saspol section. Unimodal and moderately well-sorted sediments of Unit S7 (Saspol section) is attributed to the highest and most stable lake condition. Figure 7 shows the representative frequency distribution curves and explains that in both of the sections, sediments are composed of more than one component within a grain-size distribution. Several studies describe the polymodal sediments of a lake as composed of different grain-size components within a single grain-size distribution and that each component is related to specific depositional processes (Thomas *et al.*, 1972, 1976; Ashley, 1978; Sun *et al.*, 2002; Qin *et al.*, 2005; Xiao *et al.*, 2009; Xiao, 2012, 2013). The polymodal distribution of the palaeolake shows that the sediments supplied are the result of reworked fluvial, aeolian and eroded lake margin materials.

The SK and KG are functions of internal sorting of the distribution and are related to the amount of reworking and accumulated energy (Cadigan, 1961); SK reflects the predominance of coarse or fine sediments (Folk & Ward, 1957; Friedman, 1961). In completely symmetrical distribution, mean and median diameters will coincide. However, if the sample has a widespread tail towards the fine grain-size end, the sample is positively skewed and a tail towards coarse grain size is negatively skewed. The KG denotes the ratio between the sorting in tails of the curve to that of the central portion. In this study, SK and KG show a non-normal distribution for both of the sedimentary sequences. It is seen that silt mode plays a fundamental role in modifying the symmetry of the sediments. Lithounits with a sand and clay dominant population exhibit asymmetrical distribution owing to the presence of silt in the composition. Even lithounits having discrete silt populations do not conform to normal distribution which may be due to the presence of variations in silt size range, i.e. coarse to fine silt. Clay deposits of Unit K12 (Khalsi) and Units S3, S5 and S7 (Saspol) exhibit coarse (negative) skewed values while all other units display a fine (positive) skewed value. Figures 3B and 6B show that coarse sized sediments ranging from sand to coarse silt are very fine skewed which reflects excessive riverine input. Previous studies also describe river sediments as positively skewed (Friedman, 1961, 1979; McLaren, 1981). The value of skewness decreases with fining of grain size. Negative skewness of clay deposits arises from the dominant finer mode (clay) with a coarse tail (silt) (Folk & Ward, 1957; Thomas *et al.*, 1976). Figures 3C and 6C show that most of the sediments of Saspol section are mesokurtic to leptokurtic while in Khalsi section the majority of sediments exhibit a strongly leptokurtic distribution. Sand and clay sediments are leptokurtic which shows the presence of one principal mode and a subordinate mode in the tail. The silt dominating population is mostly mesokurtic in nature. Mesokurtic distribution can result from the existence of different modes having a less differentiated size range (Folk & Ward, 1957). Extreme high and low kurtosis values as described by Folk & Ward (1957) denote that sediment has achieved its sorting in a previous high energy environment and is now transported and deposited in a new environment of less effective sorting energy, which in this case is the less efficient sorting environment of a lake. Both skewness and kurtosis thus reflect the depositional energy condition. Positive skewness shows a competency of the transporting agent compared with the negative skewed value of clay deposits and the leptokurtic nature of kurtosis indicates poor sorting of the sediment.

Basic similarities in the textural characteristics trend of both sections indicate a similarity in the source material for the sediments of Saspol and Khalsi. It is seen that sediments of the Khalsi section show a poorer degree of sorting and coarser grain size as compared with the sediments of the Saspol section, which can be attributed to the location of the sections within the lake system. Khalsi is close to the outflow of the river and is situated in the nearshore zone of the lake, implying higher depositional energy conditions, while Saspol is situated upstream of

the river and is close to the offshore zone of the lake. However, differences in their position in the lake do not alter the trend of textural characteristics of the sediment. The similar nature of the sediment character and chronology indicates that both of the sedimentary sequences were deposited in the same time period and as part of the same lake system. A lithological description of the sequences and their stratigraphic correlation is achieved on the basis of the textural properties and available chronology.

The accelerator mass spectrometer (AMS) radiocarbon dates bracket the Saspol sequence from *ca* 12·3 to *ca* 7·2 ka. The sequence starts with a silty sand bed of Unit S1. The dominant sand mode and absence of sedimentary structures indicate deposition of sediments in the waning phase of a fluvial regime. This is followed by alternate fine silt and clay beds (Unit S2) perhaps indicating a shallow phase of lacustrine sedimentation. The massive clay bed of Unit S3 implies sedimentation in low energy stagnant water conditions to allow the suspension sediment to be deposited (Fig. 5E). Mean grain size decreases from Unit S1 (average mean size 4·19 ϕ) to Unit S3 (average mean size 9·83 ϕ). Units S1, S2 and S3 together show a fining upward trend and gradual transformation from fluvial to lacustrine conditions. Unit S4 is characterized by an interlayered silt and clay bed. The coarse-grained sediment may have deposited due to some wave or current activity while the clay indicates deposition during slack water conditions. This indicates a decrease in lake level and deposition in a shelf-like setting. Recurrence of high water stand and calm depositional conditions is denoted by bedded clay of Unit S5. Units S4 and S5 together show another fining up cycle, suggesting sedimentation in a lake setting. Deposition of a coarse to medium silt bed (Unit S6) depicts the return of increasing energy conditions at the site of deposition overlain by a massive clay bed (Unit S7). The association of Units S6 and S7 (Fig. 5F) shows a third fining up sequence. Such a massive and fine-grained nature of sediment (Unit S7) points to very low energy, and accounts for the occurrence of the highest water level and a stable lake phase. Units S8 to S12 show deposition of alternate medium to fine silt and coarse to medium silt. This facies association is deposited during shoaling low water conditions of the shallow lake that caused erosion of the lake shore and deposition of alternate fine and coarse silt.

The AMS radiocarbon dates bracket the Khalsi sequence from *ca* 14·6 to *ca* 5 ka. The palaeolake sequence starts with coarse to fine silt deposits with very coarse silty partings (Unit K1) overlain by a very fine sand bed (Unit K2). Units K1 and K2 form a coarsening-upward cycle and point to an upper flow regime. A second coarsening up cycle is comprised of Unit K3 (medium to fine silt) and Unit K4 (very coarse silt). Deposition of a fine silt bed in Unit K5 followed by a coarse silt bed in Unit K6 and deposition of a cross-bedded fine sand bed in Unit K7 account for the third coarsening up sequence. These coarsening-upward trends denote occasional increases in water flow velocity and gradual switching to a dominantly fluvial setting as indicated by the channelized sand of Unit K7. Deposition of a very fine silt bed (Unit K8) marks the decrease in depositional energy conditions and an increase in water level. A fining up cycle comprising Units K9 and K10 points to the gradual drop in energy regime and deposition in a lake setting. The lowest energy condition and highest lake level with deposition of very fine silt and clay is attributed to the second fining up cycle consisting of Units K11 and K12 (Fig. 5C). Deposition of a coarse to fine silt bed (Unit K13) indicates the shallowing phase of the lake.

Based on the available chronology, a shallow fluvial environment (Unit S1 and Units K6 and K7) possibly at the end of the Younger Dryas (*ca* 12 ka) is seen. From *ca* 11 ka, an amelioration in the climate is seen as Holocene warming which is well-recorded in Unit K8 onward to Unit K12 (7 m of the Khalsi section) and Unit S3 to Unit S7 (*ca* 10 m of the Saspol section), recording the highest lake level. Earlier studies have revealed intensified monsoon activity *ca* 11·5 ka onward from Tsokar lake of the Ladakh region and Tibetan lakes (van Campo & Gasse, 1993; Fontes *et al.*, 1996; Demske *et al.*, 2009; Wünnemann *et al.*, 2010). The highest lake level is recorded from Bangong lake *ca* 9·6 to 8·7 ka (Hui *et al.*, 1996). Because the area receives winter precipitation in the form of snow by westerly disturbance, the sustenance of high water level is attributed to enhanced summer precipitation from the Indian summer monsoon and glacial meltwater as a result of Holocene warming. The high sedimentation rate of Saspol (upstream section) is more likely to be because of the contribution of sediments from the Likhir and Saspol Tokpo (Nala – small stream) entering the lake. The shallowing of the lake is seen in Unit K13 and Units S8 to S12 with a little fluctuation in Unit S11 in the Saspol section. However,

deposition in Khalsi is seen from 14·6 ka. The period from 14·6 to 11·7 ka (Units K1 to K5) shows an unstable lake condition with a drastic rise and fall in water level, being a period between the Older and Younger Dryas with an intervening warming phase.

CONCLUSIONS

From the grain-size distribution study it is seen that the lake is composed of three primary grain-size components – sand, silt and clay. Although both sections are part of the same lake system, because of their relative positions, Khalsi section deposits (located at the nearshore zone of the lake) are composed of comparatively coarser sediment when compared with Saspol section deposits (located close to the offshore zone of the lake). However, the location of the sections does not affect the trend of textural characteristics of the components, implying similar source material. Current and wave motion form the prime energy controlling the mean size and sorting, and generating the polymodal nature of the sediments. Both sections display poorest sorting in the coarse to fine silt size deposits and comparatively better sorting of sand and clay. Skewness and kurtosis reflect the depositional energy conditions. Positive skewness of sand and silt show a competency of the transporting agent compared with the negative skewed value of clay deposits. The leptokurtic nature of the sediments indicates deposition in the less efficient sorting environment of the lake while a mesokurtic distribution can result from the existence of different modes having less differentiated size ranges. Deposition of very fine silt and clay is attributed to warming of the climate and substantial monsoons causing the lake level to rise, while the coarse grain size is assigned to the comparatively colder phase when shallow water conditions existed. Thus, this study gives an idea about the sedimentation pattern of the hydrologically open valley lakes in high-altitude, cold and arid deserts. Unlike the closed basin lakes, these are long, deep and narrow with the presence of prominent offshore conditions and high energy activity directed towards the end of the basin. Silt is the key component determining the sediment character in these lakes, and the presence of silt, in the sand and clay population, gives rise to positive and negative skewness, respectively, and also produces high kurtosis values.

ACKNOWLEDGEMENTS

We sincerely thank the Director, BSIP, Lucknow for encouragement (BSIP/RDCC/65/2015-16). Laboratory facilities were provided by the Geology Department, Lucknow University, Lucknow, India. Wild Life Department, Jammu (J&K) is thanked for permission to carry out studies in the area. Two anonymous reviewers are thanked for their valuable suggestions which led to the improvement of this work.

REFERENCES

Ashley, G.M. (1978) Interpretation of polymodal sediments. *J. Geol.*, **86**, 411–421.

Bagati, T.N., **Mazari, R.K.** and **Rajagopalan, G.** (1996) Palaeotectonic implications of Lamayuru lake (Ladakh). *Curr. Sci.*, **71**, 479–482.

Bagnold, R.A. and **Barndorff-Nielsen, O.** (1980) The pattern of natural size distributions. *Sedimentology*, **27**, 199–207.

Blöthe, J.H., **Munack, H.**, **Korup, O.**, **Fulling, A.**, **Garzanti, E.**, **Resentini, A.** and **Kubik, P.W.** (2014) Late Quaternary valley infill and dissection in the Indus River, western Tibetan Plateau margin. *Quatern. Sci. Rev.*, **94**, 102–119.

Blott, S.J. and **Pye, K.** (2001) Gradistat: a grain size distribution and statistics package for the analysis of unconsolidated sediments. *Earth Surf. Proc. Land.*, **26**, 1237–1248.

Boggs, S., Jr (1995) *Principles of Sedimentology and Stratigraphy*. Prentice Hall, Englewood Cliffs, NJ.

Bookhagen, B., **Thiede, R.C.** and **Strecker, M.R.** (2005) Late Quaternary intensified monsoon phases control landscape evolution in the northwest Himalaya. *Geology*, **33**, 149–152.

Burbank, D. (1983) Multiple episodes of catastrophic flooding in the Peshawar Basin during the past 700,000 years. *Geol. Bull. Univ. Peshawar*, **16**, 43–49.

Cadigan, R.A. (1961) Geologic interpretation of grain-size distribution measurements of Colorado Plateau sedimentary rocks. *J. Geol.*, **69**, 121–144.

van Campo, E. and **Gasse, F.** (1993) Pollen and Diatom-inferred climatic and hydrological changes in Sumxi Co Basin (Western Tibet) since 13,000 yr B.P. *Quatern. Res.*, **39**, 300–313.

Chen, F., **Yu, Z.**, **Yang, M.**, **Ito, E.**, **Wang, S.**, **Madsen, D.B.**, **Huang, X.**, **Zhao, Y.**, **Sato, T.**, **Birks, H.J.B.**, **Boomer, I.**, **Chen, J.**, **An, C.** and **Wünnemann, B.** (2008) Holocene moisture evolution in arid central Asia and its out-of-phase relationship with Asian monsoon history. *Quatern. Sci. Rev.*, **27**, 351–364.

Clift, P.D. (2002) A brief history of the Indus River. *J. Geol. Soc. London*, **195**, 237–258.

Demske, D., **Tarasov, P.E.**, **Wünnemann, B.** and **Riedel, F.** (2009) Late glacial and Holocene vegetation, Indian monsoon and westerly circulation dynamics in the Trans-Himalaya recorded in the pollen profile from high-altitude Tso Kar Lake, Ladakh, NW India. *Palaeogeogr. Palaeoclimatol. Palaeoecol.*, **279**(3–4), 172–185.

Folk, R.L. (1966) A review of grain-size parameters. *Sedimentology*, **6**, 73–93.

Folk, R.L. (1974 *Petrology of Sedimentary Rocks*. Hemphill, Austin, TX, 182 pp.

Folk, R.L. and **Ward, W.C.** (1957) Brazos River Bar: a study in the significance of grain size parameters. *J. Sed. Petrol.*, **27**, 3–26.

Fontes, J.C., **Gasse, F.** and **Gilbert, E.** (1996) Holocene environmental changes in Lake Bangong basin (Western Tibet). Part 1: chronology and stable isotopes of carbonates of a Holocene lacustrine core. *Palaeogeogr. Palaeoclimatol. Palaeoecol.*, **120**, 25–47.

Fort, M., **Burbank, D.W.** and **Freytet, P.** (1989) Lacustrine sedimentation in a semi-arid alpine setting: an example from Ladakh, northwestern Himalaya. *Quatern. Res.*, **31**, 332–352.

Friedman, G.M. (1961) Distinction between dune, beach and river sands from their textural characteristics. *J. Sed. Petrol.*, **31**, 514–529.

Friedman, G.M. (1979) Differences in size distributions of populations of particles among sands of various origins. *Sedimentology*, **26**, 3–32.

Garzanti, E. and **Van Haver, T.** (1988) The Indus clastics: forearc basin sedimentation in the Ladakh Himalaya (India). *Sed. Geol.*, **59**, 237–249.

Gasse, F., **Arnold, M.**, **Fontes, J.C.**, **Fort, M.**, **Gilbert, E.**, **Huc, A.**, **Li, B.**, **Li, Y.**, **Qing, L.**, **Mélières, F.**, **van Campo, E.**, **Fubao, W.** and **Qingsong, Z.** (1991) A 13000-year climate record from western Tibet. *Nature*, **353**, 742–745.

Gasse, F., **Fontes, J.C.**, **van Campo, E.** and **Wei, K.** (1996) Holocene environmental changes in Bangong Co basin (Western Tibet). Part 4: discussion and conclusions. *Palaeogeogr. Palaeoclimatol. Palaeoecol.*, **120**, 79–92.

Gierlowski-Kordesch, E. and **Kelts, K.** (2000) *Lake Basins Through Space and Time*. AAPG, Tulsa, OK.

Glaister, R.P. and **Nelson, H.W.** (1974) Grain-size distributions, an aid in facies identification. *Bull. Can. Petrol. Geol.*, **22**, 203–240.

Gu, Z., **Liu, J.**, **Yuan, B.**, **Liu, T.**, **Liu, R.**, **Liu, Y.** and **Zhang, G.** (1993) The changes in monsoon influence in the Qinghai-Tibetan Plateau during the past 12,000 years. Geochemical evidence from the L. Selin sediments. *Chin. Sci. Bull.*, **38**, 61–64.

Håkanson, L. and **Jansson, M.** (1983) *Principles of Lake Sedimentology*. Springer-Verlag, Berlin.

Hewitt, K. (1982) Natural dams and outburst floods of the Karakoram Himalaya. *IAHS Publ. No.*, **138**, 259–269.

Hui, F., **Gasse, F.**, **Huc, A.**, **Yuanfang, L.**, **Sifeddine, A.** and **Soulié-Märsche, I.** (1996) Holocene environmental changes in Bangong Co basin (western Tibet). Part 3: biogenic remains. *Palaeogeogr. Palaeoclimatol. Palaeoecol.*, **120**, 65–78

Inman, D.L. and **Chamberlain, D.K.** (1955) Particle-size distribution in nearshore sediments in Finding ancient shorelines. *Soc. Econ. Palaeontol. Min. Spec. Publ.*, **3**, 99–105.

Kong, P., **Na, C.**, **Brown, R.**, **Fabel, D.**, **Freeman, S.**, **Xiao, W.** and **Wang, Y.** (2011) Cosmogenic 10 Be and 26 Al dating of palaeolake shorelines in Tibet. *J. Asian Earth Sci.*, **41**, 263–273.

Kotlia, B.S. and **Rawat, K.S.** (2004) Soft sediment deformation structures in the Garbyang palaeolake: evidence for the past shaking events in the Kumaun Tethys Himalaya. *Curr. Sci.*, **876**, 377–379.

Kotlia, B.S., **Bhalla, M.S.**, **Sharma, C.**, **Rajagopalan, G.**, **Ramesh, R.**, **Chauhan, M.S.**, **Mathur, P.D.**, **Bhandari, S.** and **Chacko, S.T.** (1997a) Palaeoclimatic conditions in the upper Pleistocene and Holocene Bhimtal-Naukuchiatal lake basin in south-central Kumaun, North India. *Palaeogeogr. Palaeoclimatol. Palaeoecol.*, **130**, 307–322.

Kotlia, B.S., **Shukla, U.K.**, **Bhalla, M.S.**, **Mathur, P.D.** and **Pant, C.C.** (1997b) Quaternary fluvio-lacustrine deposits of the Lamayuru basin, Ladakh Himalaya: preliminary multidisciplinary investigations. *Geol. Mag.*, **134**, 807–815.

Kotlia, B.S., **Bhalla, M.S.**, **Shah, N.** and **Rajagopalan, G.** (1998) Palaeomagnetic results from the Pleistocene-Holocene lake deposits of Bhimtal and Bhowali (Kumaun Himalaya) and Lamayuru (Ladakh Himalaya) with reference to the reversal events. *J. Geol. Soc. India*, **51**, 7–20.

Lee, J., **Li, S.** and **Aitchison, J.C.** (2009) OSL dating of palaeoshorelines at Lagkor Tso, western Tibet. *Quatern. Geochronol.*, **4**, 335–343.

Lehmkuhl, F. and **Haselein, F.** (2000) Quaternary palaeoenvironmental change on the Tibetan Plateau and adjacent areas (Western China and Western Mongolia). *Quatern. Int.*, **65**, 121–145.

Long, H., **Lai, Z.P.**, **Wang, N.A.** and **Li, Y.** (2010) Holocene climate variations from Zhuyeze terminal lake records in East Asian monsoon margin in arid northern China. *Quatern. Res.*, **74**, 46–56.

Long, H., **Lai, Z.P.**, **Fuchs, M.**, **Zang, Z.R.** and **Li, Y.** (2012) Timing of Late Quaternary palaeolake evolution in Tengger Desert of northern China and its possible forcing mechanisms. *Global Planet. Change*, **92**, 119–129.

Mason, K. (1929) Indus floods and Shyock glaciers. *Himalayan J.*, **1**, 10–29.

Mason, C.C. and **Folk, R.L.** (1958) Differentiation of beach, dune and aeolian flat environments by size analysis, Mustang Island, Texas. *J. Sed. Petrol*, **28**, 211–226.

McLaren, P. (1981) An interpretation of trends in grain size measures. *J. Sed. Petrol.*, **51**, 611–624.

Mishra, P.K., **Prasad, S.**, **Anoop Plessen, B.**, **Jehangir, A.**, **Gaye, B.**, **Menzel, P.**, **Weise, S.M.** and **Yousuf, A.R.** (2015) Carbonate isotopes from high altitude Tso Moriri Lake (NW Himalayas) provide clues to late glacial and Holocene moisture source and atmospheric circulation changes. *Palaeogeogr. Palaeoclimatol. Palaeoecol.*, **425**, 76–83.

Mohindra, R. and **Bagati, T.N.** (1996) Seismically induced soft-sediment deformation structure (seismites) around Sumdo in the lower Spiti valley (Tethys Himalaya). *Sed. Geol.*, **101**, 69–83.

Mügler, L., **Gleixner, G.**, **Gunther, F.**, **Mäusbacher, R.**, **Daut, G.**, **Schütt, B.**, **Berking, J.**, **Schwalb, A.**, **Schwark, L.**, **Xu, B.**, **Yao, T.**, **Zhu, L.** and **Yi, C.** (2010) A multi-proxy approach to reconstruct hydrological changes and Holocene climate development of Nam Co, Central Tibet. *J. Palaeolimnol.*, **43**, 625–648.

Nag, D. and **Phartiyal, B.** (2015) Climatic variations and geomorphology of the Indus River Valley, between Spituk and Batalik, Ladakh (NW Trans Himalayas) in Late Quaternary. *Quatern. Int.*, **371**, 87–101.

Peng, Y., **Xiao, J.**, **Nakamura, T.**, **Liu, B.** and **Inouchi, Y.** (2005) Holocene East Asian monsoonal precipitation pattern revealed by grain-size distribution of core sediments of Daihai lake in Inner Mongolia of north-central China. *Earth Planet. Sci. Lett.*, **233**, 467–479.

Phartiyal, B. and **Sharma, A.** (2009) Soft-sediment deformation structures in the Late Quaternary sediments of Ladakh: evidence for multiple phases of seismic tremors in the North western Himalayan Region. *J. Asian Earth Sci.*, **34**, 761–770.

Phartiyal, B., **Sharma, A.**, **Upadhyay, R.**, **Ram-Awatar, SA** and **Sinha, A.K**. (2005) Quaternary geology, tectonics and distribution of palaeo- and present fluvio/glacio lacustrine deposits in Ladakh, NW Indian Himalaya – a study based on field observations. *Geomorphology* **65**, 241–256.

Phartiyal, B., **Sharma, A.** and **Kothyari, G.C.** (2013) Existence of Late Quaternary and Holocene lakes along the River Indus in Ladakh Region of Trans Himalaya, NW India: implications to climate and tectonics. *Chin. Sci. Bull.*, **58**, 142–155.

Phartiyal, B., **Singh, R.** and **Kothyari, G.C.** (2015) Late-Quaternary geomorphic scenario due to changing depositional regimes in the Tangtse Valley, Trans-Himalaya, NW India. *Palaeogeogr. Palaeoclimatol. Palaeoecol.*, **422**, 11–24.

Piotrowska, N. (2013) Status report of AMS sample preparation laboratory at GADAM Centre, Gliwice, Poland. *Nucl. Instrum. Meth. Phys. Res.*, **294**, 176–181.

Qin, X.G., **Cai, B.G.** and **Liu, T.S.** (2005) Loess record of the aerodynamic environment in the East Asia monsoon area since 60,000 years before present. *J. Geophys. Res.*, **110**, B01204. doi:10.1029/2004JB003131.

Reading, H.G. and **Levell, B.K**. (1996) Controls on the sedimentary rock record. In: *Sedimentary Environments: Processes, Facies and Stratigraphy* (Ed. H.G. Reading), 3rd edn, pp 5–35. Blackwell Science, Oxford.

Reimer, P.J., **Baillie, M.G.L.**, **Bard, E.**, **Bayliss, A.**, **Beck, J.W.**, **Bertrand, C.J.H.**, **Blackwell, P.G.**, **Buck, C.E.**, **Burr, G.S.**, **Cutler, K.B.**, **Damon, P.E.**, **Edwards, R.L.**, **Fairbanks, R.G.**, **Friedrich, M.**, **Guilderson, T.P.**, **Hogg, A.G.**, **Hughen, K.A.**, **Kromer, B.**, **McCormac, G.**, **Manning, S.**, **Ramsey, C.B.**, **Reimer, R.W.**, **Remmele, S.**, **Southon, J.R.**, **Stuiver, M.**, **Talamo, S.**, **Taylor, F.W.**, **Plicht, J.** and **Weyhenmeyer, C.E.** (2009) INTCAL04 terrestrial radiocarbon age calibration, 0–26 cal kyr BP. *Radiocarbon*, **46**, 1029–1058.

Reineck, E.H. and **Singh, I.B.** (1973) *Depositional Sedimentary Environments*. Springer-Verlag, New York, NY.

Sahu, B.K. (1964) Depositional mechanisms from the size analysis of clastic sediments. *J. Sed. Petrol.*, **34**, 73–83.

Sangode, S.J. and **Bagati, T.N.** (1995) Tectono-climatic signatures in higher Himalayan lakes: a palaeomagnetic rock magnetic approach in the lacustrine sediments of Lamayuru, Ladakh, India. *J. Him. Geol.*, **6**, 51–60.

Sangode, S.J., **Phadtare, N.R.**, **Meshram, D.C.**, **Rawat, S.** and **Suresh, N.** (2011) A record of lake outburst in the Indus valley of Ladakh Himalaya, India. *Curr. Sci.*, **100**, 1712–1718.

Sangode, S.J., **Rawat, S.**, **Meshram, D.C.**, **Phadtare, N.R.** and **Suresh, N.** (2013) Integrated mineral magnetic and lithologic studies to delineate dynamic modes of depositional conditions in the Leh valley Basin, Ladakh Himalaya, India. *J. Geol. Soc. India*, **82**, 107–120.

Sant, D.A., **Wadhwan, S.K.**, **Ganjoo, R.K.**, **Basavaiah, N.**, **Sukumaran, P.** and **Bhattacharya, A.S.** (2011) Linkage of paraglacial processes from last glacial to recent inferred from Spituk sequence, Leh valley, Ladakh Himalaya. *J. Geol. Soc. India*, **78**, 147–156.

Searle, M.P. (1986) Structural evolution and sequence of thrusting in the High Himalayan, Tibetan-Tethys and Indus suture zones of Zanskar and Ladakh, Western Himalaya. *J. Struct. Geol.*, **8**, 923–936.

Searle, M.P., **Pickering, K.T.** and **Cooper, D.J.W.** (1990) Restoration and evolution of the intermontane Indus molasse basin, Ladakh Himalaya, India. *Tectonophysics*, **174**, 301–314.

Shukla, U.K., **Kotlia, B.S.** and **Mathur, P.D.** (2002) Sedimentation pattern in a trans-Himalaya Quaternary lake at Lamayuru (Ladakh), India. *Sed. Geol.*, **148**, 405–424.

Sinclair, H.D. and **Jaffey, N.** (2001) Sedimentology of the Indus Group, Ladakh, northern India: implications for the timing of initiation of the palaeo-Indus River. *J. Geol. Soc. London*, **158**, 151–162.

Singh, S. and **Jain, A.K.** (2007) Liquefaction and fluidization of lacustrine deposits from Lahaul-Spiti and Ladakh Himalaya: geological evidences of palaeoseismicity along active fault zone. *Sed. Geol.*, **196**, 47–57.

Singh, D.S., **Gupta, A.K.**, **Sangode, S.J.**, **Clemens, S.C.**, **Prakasam, M.**, **Srivastava, P.** and **Prajapati, S.K**. (2015) Multiproxy record of monsoon variability from the Ganga Plain during 400-1200 A.D. *Quatern. Int.*, **371**, 157–163.

Sly, P.G. (1978) Sedimentary processes in lakes. In: *Lakes: Chemistry, Geology, Physics* (Ed. A. Lerman), pp. 65–89. Springer, New York, NY.

Spencer, D.W. (1963) The interpretation of grain size distribution curves of clastic sediments. *J. Sed. Petrol.*, **33**, 180–190.

Sun, D., **Bloemendal, J.**, **Rea, D.K.**, **Vandenberghe, J.**, **Jiang, F.**, **An, Z.** and **Su, R.** (2002) Grain-size distribution function of polymodal sediments in hydraulic and aeolian environments and numerical partitioning of the sedimentary components. *Sed. Geol.*, **152**, 263–277.

Thakur, V.C. (1981) Regional framework and geodynamic evolution of the Indus Tsangpo Suture Zone in the Ladakh Himalaya. *Trans. R. Soc. Edinb.*, **72**, 89–97.

Thomas, R.L., **Kemp, A.L.W.** and **Lewis, C.F.M.** (1972) Distribution, composition and characteristics of the surficial sediments of Lake Ontario. *J. Sed. Petrol.*, **42**, 66–84.

Thomas, R.L., **Jaquet, J.M.**, **Kemp, A.L.W.** and **Lewis, C.F.M.** (1976) Surficial sediments of Lake Erie. *J. Fish. Res. Board Can.*, **33**, 385–403.

Udden, J.A. (1914) Mechanical composition of clastic sediments. *Bull. Geol. Soc. Am.*, **25**, 655–744.

Visher, G.S. (1969) Grain size distribution and depositional processes. *J. Sed. Petrol.*, **39**, 1074–1106.

Wang, S.M. and **Dou, H.S.** (1998) *Records of Lakes in China*. Science Press, Beijing.

Wei, K. and **Gasse, F.** (1999) Oxygen isotopes in lacustrine carbonates of West China revisited: implications for post glacial changes in summer monsoon circulation. *Quatern. Sci. Rev.*, **18**, 1315–1334.

Wu, Y., **Lucke, A.**, **Jin, Z.**, **Wang, S.**, **Schleser, G.H.**, **Battarbee, R.W.** and **Xia, W.** (2006) Holocene climate development on the central Tibetan Plateau: a sedimentary record from Cuoe Lake. *Palaeogeogr. Palaeoclimatol. Palaeoecol.*, **234**, 328–340.

Wünnemann, B., **Demske, D.**, **Tarasov, P.**, **Kotlia, B.S.**, **Reinhardt, C.**, **Bloemendal, J.**, **Diekmann, B.**, **Hartmann, K.**, **Krois, J.**, **Riedel, F.** and **Arya, N.** (2010) Hydrological evolution during the last 15 kyr in the Tso Kar lake basin (Ladakh, India), derived from geomorphological, sedimentological and palynological records. *Quatern. Sci. Rev.*, **29**, 1138–1155.

Xiao, J. (2012) The link between grain-size components and depositional processes in a modern clastic lake. *Sedimentology*, **59**, 1050–1062.

Xiao, J. (2013) A model for linking grain-size component to lake level status of a modern clastic lake. *J. Asian Earth Sci.*, **69**, 149–158.

Xiao, J., **Chang, Z.**, **Si, B.**, **Qin, X.**, **Itoh, S.** and **Lomtatidze, Z.** (2009) Partitioning of the grain-size components of Dali Lake core sediments: evidence for lake-level changes during the Holocene. *J. Palaeolimnol.*, **42**, 249–260.

Zhao, X., **Zhu, D.**, **Yan, F.**, **Wu, Z.**, **Ma, Z.** and **Mai, X.** (2003) Climatic change and lake-level variation of Nam Co, Xizang since the last interglacial stage. *Quatern. Sci.*, **23**, 41–52.

Zheng, M., **Yuan, H.**, **Zhao, X.** and **Liu, X.** (2006) The Quaternary Pan-lake (overflow) period and palaeoclimate on the Qinghai-Tibet Plateau. *Acta Geol. Sinica*, **80**, 169–180.

Manuscript received 30 October 2015; revision accepted 7 April 2016